climate

MDPI

Homogenous Climatic Regions for Targeting Green Water Management Technologies in the Abbay Basin, Ethiopia

Degefie Tibebe [1,2], Mekonnen Adnew Degefu [1,3,*], Woldeamlak Bewket [1,4], Ermias Teferi [1,5], Greg O'Donnell [6] and Claire Walsh [6]

[1] Water and Land Resource Center (WLRC), Addis Ababa University, Addis Ababa P.O. Box 3880, Ethiopia; d.tibebe@cgiar.org (D.T.); woldamlak.b@wlrc-eth.org (W.B.); ermias.t@wlrc-eth.org (E.T.)
[2] Alliance Bioversity International and International Center for Tropical Agriculture (CIAT), Addis Ababa P.O. Box 5689, Ethiopia
[3] Department of Geography and Environmental Studies, Debre Markos University, Debre Markos P.O. Box 269, Ethiopia
[4] Department of Geography & Environmental Studies, Addis Ababa University, Addis Ababa P.O. Box 1176, Ethiopia
[5] Center for Environment and Development, Addis Ababa University, Addis Ababa P.O. Box 3880, Ethiopia
[6] School of Engineering, Newcastle University, Newcastle upon Tyne NE1 7RU, UK; g.m.o'donnell@newcastle.ac.uk (G.O.); claire.walsh@ncl.ac.uk (C.W.)
* Correspondence: author: mekonnen.a@wlrc-eth.org

Abstract: Spatiotemporal climate variability is a leading environmental constraint to the rain-fed agricultural productivity and food security of communities in the Abbay basin and elsewhere in Ethiopia. The previous one-size-fits-all approach to soil and water management technology targeting did not effectively address climate-induced risks to rain-fed agriculture. This study, therefore, delineates homogenous climatic regions and identifies climate-induced risks to rain-fed agriculture that are important to guide decisions and the selection of site-specific technologies for green water management in the Abbay basin. The k-means spatial clustering method was employed to identify homogenous climatic regions in the study area, while the Elbow method was used to determine an optimal number of climate clusters. The k-means clustering used the Enhancing National Climate Services (ENACTS) daily rainfall, minimum and maximum temperatures, and other derived climate variables that include daily rainfall amount, length of growing period (LGP), rainfall onset and cessation dates, rainfall intensity, temperature, potential evapotranspiration (PET), soil moisture, and AsterDEM to define climate regions. Accordingly, 12 climate clusters or regions were identified and mapped for the basin. Clustering a given geographic region into homogenous climate classes is useful to accurately identify and target locally relevant green water management technologies to effectively address local-scale climate-induced risks. This study also provided a methodological framework that can be used in the other river basins of Ethiopia and, indeed, elsewhere.

Keywords: climate homogenization; k-means clustering; green water; technology targeting; abbay basin

1. Introduction

Spatiotemporal climate variability is a leading environmental factor that determines the rain-fed agricultural productivity and food security of communities in a given geographical region by affecting the amount and spatiotemporal distribution of green water resources; the water held in the soil and available to crops and plants [1,2]. The effect of temperature and rainfall variability causes inter-annual variability in cereal crop productivity by about 30–50% in rain-fed agriculture [3]. The impact of climate variability is extremely high in countries like Ethiopia, where there is very high spatiotemporal rainfall and temperature variability caused by the complex topography and north–south oscillation

of overhead solar radiation [4]. An annual-based north–south oscillation of overhead solar radiation over Ethiopia determines the location of the Inter Tropical Convergence Zone (ITCZ), then by the direction and magnitude of rain-producing wind flow [4]. The impact of climate on rain-fed agriculture is not only caused by inter-annual rainfall variability but also by fluctuations in annual rainfall cycles, length of growing period (LGP), rainfall intensity, rainfall onset and cessation dates, and outbreaks of climate-related crop diseases and pests [5–7]. Temperature also determines the spatial and temporal distribution of green water and crop productivity in the rain-fed agriculture system by influencing the rate of water loss from the soil through evapotranspiration [7,8].

Evidence from empirical studies such as [4] indicates that the occurrence and impact of climate-induced risks on rain-fed agriculture differ from region to region significantly. Furthermore, except for temperature, which showed a steadily increasing trend over large areas, trends in rainfall amount and extremes are complex and varied from place to place in the Abbay basin in particular and across Ethiopia in general [4,9]. Similarly, scenario-based studies indicate that the impacts of future climate change on rain-fed agriculture and crop productivity vary from place to place in Ethiopia [10,11]. In addition to the climatic factors, there are other environmental factors such as topography, soil condition, land use, and cover, as well as anthropogenic factors such as agricultural practices and management decisions that can affect the availability of green water in a given area and at a particular time [12]. Recent evidence also confirms that climate change, population growth, and land cover conversation are significantly affecting the availability and distribution of green water resources [13–15].

Poor water utilization and management practices are another set of drivers for the low productivity of primary smallholder rain-fed agriculture in the county [16]. Although many soil and water conservation programs and projects have been implemented since the 1980s, the outcomes have not been adequate nor sustainable as both design and implementations followed top-down and one-size-fits-all approaches without considering spatial climatic variations [16,17]. Moreover, the traditional agroecological zone (AEZ)-based recommendations for green water and agronomic management practices [18] poorly capture local-scale climate-driven green water-related risks. Hence, there is a need to improve green water management practices and the targeting of green water management interventions in the country by considering local scale patterns and risks of climate variability and climate change. Clustering areas into homogenous climatic units can facilitate the identification and characterization of major agricultural water security risks, as well as foster the selection and implementation of site-specific green water management technologies [16].

BCEOM [19] is the only available study that has classified the Abbay basin into four climate clusters by considering the spatial variation of rainfall amount and its seasonal distribution. The four climate clusters include (1) the southeastern part of the basin, which receives more than 1400 mm mean annual rainfall and has a relatively longer monomodal rainfall pattern; (2) the central part of the basin which is characterized by short-length monomodal rainfall pattern; (3) the eastern part of the basin that has small and bimodal rainfall pattern; and (4) the northwestern part of the basin that has monomodal rainfall pattern and receives less than 1200 mm mean annual rainfall amount. Another national-scale study conducted by [20] classified the Abbay basin into five rainfall clusters based on seasonal rainfall cycles and interannual rainfall variability. These rainfall-based clustering studies have identified the broader regional classes but have not captured local scale rainfall variability and water availability and, hence, are not suitable for local scale planning and operational activities. There is a need for a higher resolution classification that uses multiple climate and non-climate (e.g., topography) variables to support effective green water management.

The objective of this study is to produce and characterize climate clusters for the Abbay basin. The clustering was made for the *kiremt* (June–September) primary rainy season, which supports 70–80% of the rain-fed agricultural production of the country. Different from previous studies such as [19,21–24] that considered only the spatial variation of the

annual rainfall cycle, we used other rainfall variables (rainfall amount, onset and cessation dates, length of growing period, and rainfall intensity), temperature, evapotranspiration, and soil moisture in our climate classification. These climate variables are important determinants of the productivity of the rain-fed agricultural system of the country [25–29]. The results generated from this study are useful to optimize the selection and application of site-specific green water management technologies in the study area.

2. Data and Methods

2.1. Study Area

The Abbay basin, also called the Upper Blue Nile Basin (UBNB), is located in the northwestern part of Ethiopia between 7°40′ N and 12°51′ N and 34°25′ E and 39°49′ E and covers a total area of 199,812 km^2 (Figure 1). Rugged topography in the central and eastern parts and flat lowlands in the western parts is the major terrain feature of the basin. About 60% of the basin's area is highland, with elevations of ≥1500 m asl. It is an important basin in the country as it contributes approximately 45% of the total surface water resources, accommodates 25% of the population, accounts for 20% of the area, and contributes about 40% of the agricultural production in the country [30]. The mean annual runoff generated from the Abbay basin is estimated at 49 BCM. The rugged topography, together with the north–south oscillation of the Inter Tropical Convergence Zone (ITCZ), controls the geographical and temporal distribution of the climate system in the Abbay basin [31]. The climate in the Abbay basin varies between hot and semi-arid conditions in the lowlands along the Ethio-Sudanese border and cool and humid conditions in the highlands located in the eastern part of the basin [32].

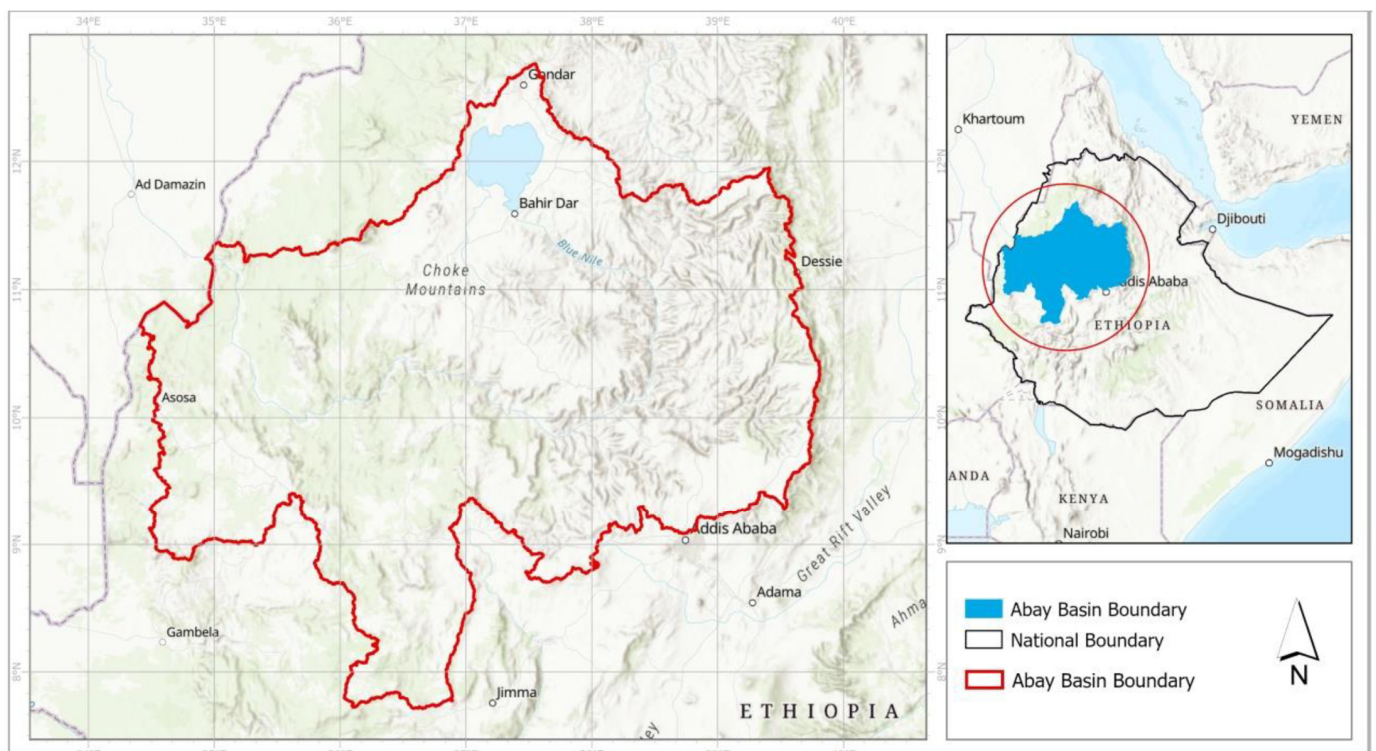**Figure 1.** Map of Abbay River basin.

2.2. Data and the Sources

For this study, different climatic data were used for processing and development of homogeneous climate clusters (Table 1). The Enhancing National Climate Services (EN-ACTS) daily time scale 4 km resolution rainfall and minimum and maximum temperature datasets [33] were used. These datasets were also used to derive the onset date, cessation

date, and length of growing period (LGP), which were used as inputs in the analysis. Climate variability controls the practice and productivity in the rain-fed agricultural system by determining the start and end of the farming calendar, LGP, soil moisture balance, and types of crops that can be grown in an area [5,6].

Table 1. Data used for climatic regionalization in the Abbay basin.

No	Data Type	Source	Spatial Resolution	Temporal Resolution
1	Precipitation	ENACTS	~4 km	1981–2018 (daily)
2	Maximum temperature (Tmax)	ENACTS	~4 km	1981–2018 (daily)
3	Minimum temperature (Tmin)	ENACTS	~4 km	1981–2018 (daily)
4	Onset date	Own analysis	~4 km	1981–2018 (Annual)
5	Cessation	Own analysis	~4 km	1981–2018 (Annual)
6	Length of growing period (LGP)	Own analysis	~4 km	1981–2018 (Annual)
7	Potential evapotranspiration (PET)	Own analysis	~4 km	1981–2018 (daily)
8	Precipitation Concentration Index (PCI)	Own analysis	~4 km	1981–2018 (Annual)
9	Soil moisture	Own analysis	~4 km	1981–2018 (daily)
10	Elevation	AsterDEM v2		

The rainfall onset and cessation dates were defined using a modified version of the Food and Agricultural Organization (FAO, 1986) method. It was defined as the day n after 1 June (i) or 1 March (i), depending on the season, when the daily precipitation exceeds half of the potential evapotranspiration.

$$\sum_{i=1}^{n} R > \sum_{i=1}^{n} PET/2$$

Rainfall cessation was defined as the period when this relationship no longer holds. It is important to mention here that the indicated cessation dates do not mean that there is no rainfall after those dates; rather, the cessation dates refer to the dates when the amount of rainfall becomes less than half of the PET. The length of the growing season (LGP) is simply defined as the number of days between the onset and cessation. The rainfall onset, cessation, and LGP computations were performed for two rainy seasons, which occurred during June–July–August–September (JJAS) and March–April–May (MAM). Most parts of the study area received rainfall during JJAS; however, some areas received short rain during MAM, apart from the JJAS. Potential evapotranspiration was computed using the Hargreaves method, considering the daily minimum and maximum temperature from the ENACT dataset. Soil moisture was estimated using a simple bucket 1D water balance model at the daily timescale and was used as the input. In this method, soil moisture was generated at the daily timescale by assuming the soil to be a reservoir that periodically fills by rainfall events in the form of randomly distributed patterns [34]. This water balance mode was used to estimate soil moisture dynamics in a single top soil layer and conceptualized as a bucket receiving and filled by infiltration driven by gravity and lost by evapotranspiration and/or drainage [35]. The precipitation concentration index was generated from the precipitation data and used to capture the temporal distribution of rainfall and its spatial pattern. It is used to quantify the relative distribution of rainfall patterns. According to Oliver [36], a PCI value < 10.0 represents a mostly uniform precipitation distribution. A PCI between 11 and 15 represents moderate precipitation concentration. A PCI between 16 and 20 represents an irregular distribution. A PCI value above 20 represents strong irregularity.

Topography is another dimension that was considered in the study since it is an important local climate modifier as well as determines surface moisture conditions. Overall, 10 variable input layers were prepared for the clustering analysis (Table 1).

2.3. Data Processing

A stepwise data processing technique was employed for the study (Figure 2). The first step was making all data layers have the same boundary and spatial resolution; the

data layers were clipped to the Abbay basin boundary and resampled to a 4 km grid resolution. The second step involved the calculation of exceedance probabilities to capture the temporal variability of the climate variables. The exceedance probability indicates the likelihood that up to a certain value occurs based on historical data. Typically, an 80% exceedance probability is used in long-term climate analysis, and this reference was used here. Subsequent to the exceedance probabilities computation, variable selection was carried out to reduce the variable space and allow parsimonious model-based clustering. For this, principal component analysis (PCA) was used to reduce the data dimension and maintain only important variables by excluding those that carry redundant information. PCA axes with eigenvalues greater than 1 were retained to ensure that only PCA axes with a significant contribution were used for further analysis [37]. However, we retained a climate variable (cessation date) due to its importance in determining the timing and availability of green water resources in the rain-fed agricultural system. The final data processing step was clustering, and in this study, the k-means spatial clustering [38–41] was employed to find homogenous climatic regions of the study area. k-means clustering is generally simple to implement, and it can be used with large datasets having medium to coarse spatial resolution.
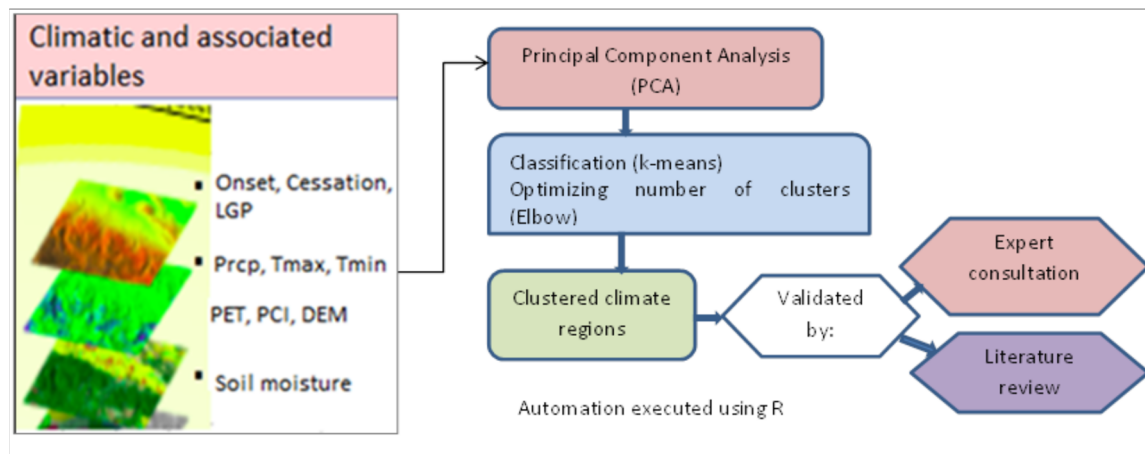

Figure 2. General framework of clustering.

k-means clustering is defined as the sum of squared distances of Euclidean distances between items and the corresponding centroid, which is shown as follows:

$$W(C_k) = \sum_{x_i \in C_k} (Xi - \mu k)^2$$

Here, xi is the ith data point of cluster k (C_k), and μk is the mean value of points in cluster k. The total within-cluster variation is defined as follows:

Total within-cluster variation =

$$\sum_{k=1}^{k} W(C_k) = \sum_{k=1}^{k} \sum_{x_i \in C_k} (Xi - \mu k)^2$$

The total within-cluster sum of squares measures the goodness of the clustering, which increases as the sum of squares measures decreases.

The k-means algorithm requires the user to specify the number of clusters. To reduce subjectivity, the elbow method was used to select the optimal number of clusters. The Elbow method helps to find the optimal number of clusters. This method uses the concept

of Within Cluster Sum of Squares (WCSS), which defines the total variations within a cluster. WCSS is calculated with the following formula:

$$WCSS = \sum P_{i\ in\ cluster\ 1}\ distance\ (P_i\ C_1\ )^2 + P_{i\ in\ cluster\ 2}\ distance\ (P_i\ C_2\ )^2$$
$$+ P_{i\ in\ cluster\ 3}\ distance\ (P_i\ C_3\ )^2$$

In the formula of WCSS, $\sum P_{i\ in\ cluster\ 1}\ distance\ (P_i\ C_1\ )^2$ is the sum of the square of the distances between each data point and its centroid within cluster 1. To measure the distance between data points and the centroid, Euclidean distance or Manhattan distance can be used. The elbow method uses a graphical representation to select the optimal K.

The 1st moment and 2nd moment descriptive statistics were applied to characterize each homogeneous climate cluster and interpret it with respect to water availability and agricultural water management. In this regard, mean, median, range, standard deviation, and variance statistics were used. The climate classification was performed for the *Kiremt* growing season. The length of the growing period (LGP) was defined as the number of days taken for the cumulative precipitation to exceed half the cumulative potential evapotranspiration. The rainfall onset and cessation dates were also determined by considering this water balance approach.

3. Results

3.1. Variables Used for Clustering

The variables used for the clustering were selected by applying PCA. The variance, cumulative variance, and Eigenvalues generated from the PCA are shown in Figure 3. The result reveals that the two components with an Eigenvalue greater than one explain more than 77% of the variance. Of this, 52.3% of the variance was explained by the first component, and the remaining 25.2% of the variance was explained by the second component. The Eigenvalues after the second dimension are less than one, indicating that these PCs explain less than the original variables (Figure 3). Accordingly, only the first and second principal components were retained and selected for further analysis.
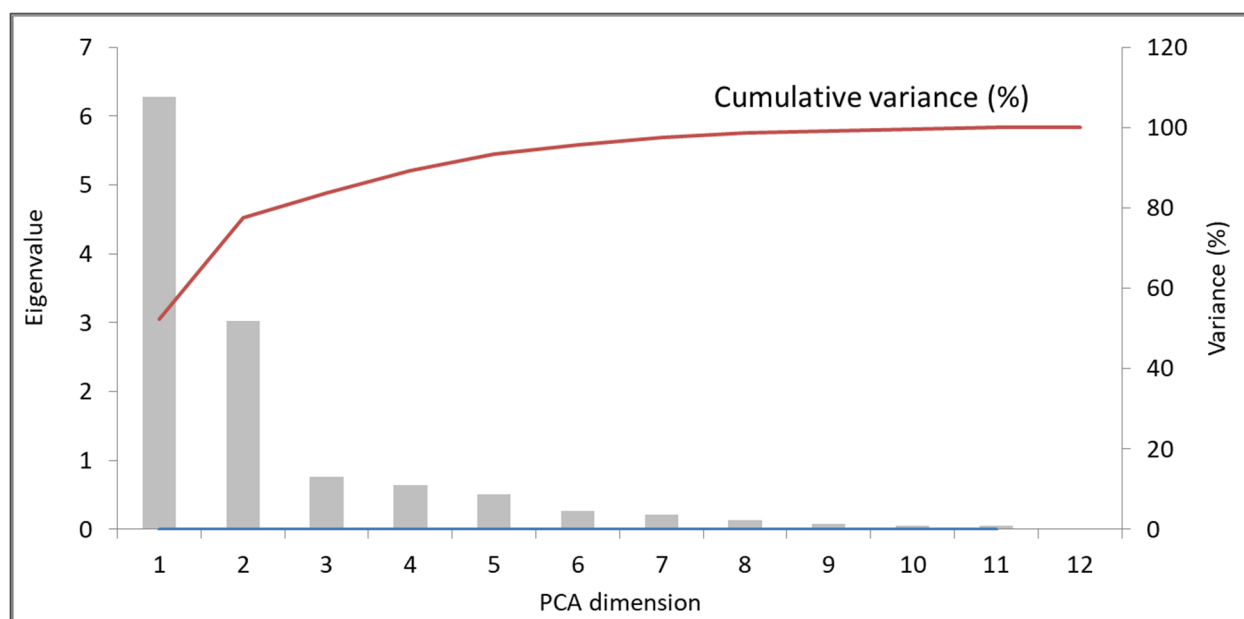

Figure 3. PCA dimensions, Eigenvalue, and cumulative variance.

The quality of variable representation was analyzed and demonstrated on a Cos2 factor map (Figure 4). The results are presented in the Cos2 factor map, on which the variables that are better represented by the two PCs appear close to the circumference of

the correlation circle. The variables are well represented by the principal components, with the exception of the rainfall cessation date, which has a lower representation. This latter variable was kept in the analysis due to its importance for agriculture.
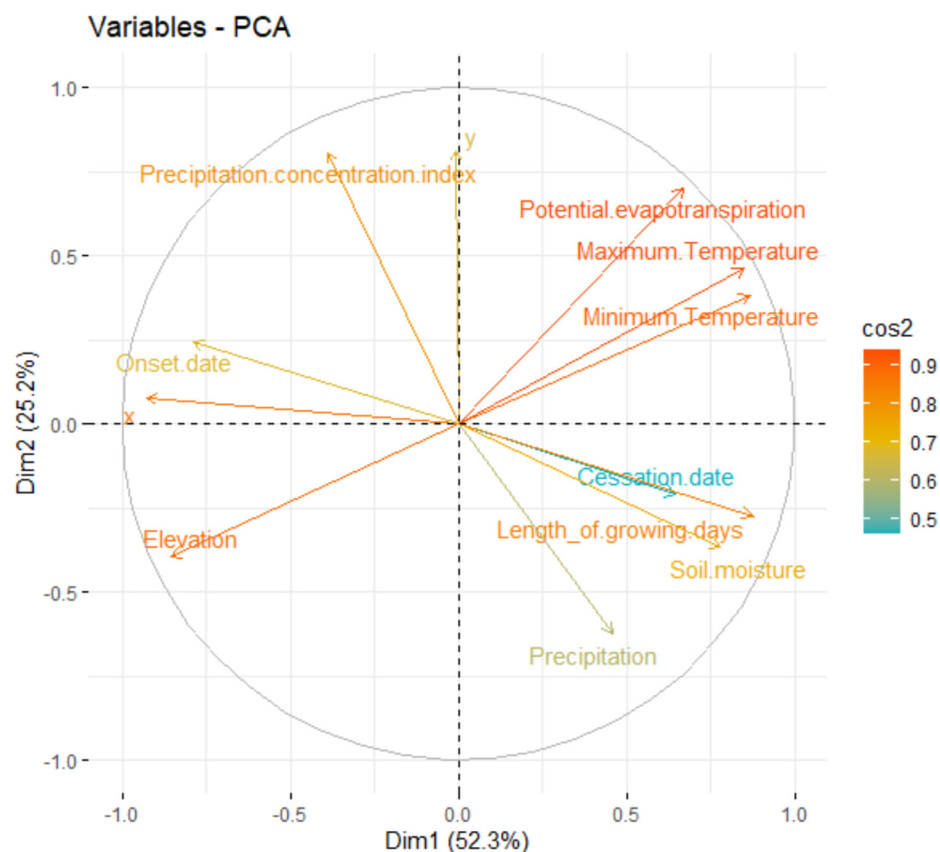

Figure 4. Cos2 factor map representing the quality of variables.

The result shows that the elevation, length of growing season, rainfall onset date, maximum and minimum temperatures, soil moisture, and potential evapotranspiration contribute the most to dimension one, while the precipitation concentration index, PET, and precipitation contribute to dimension two. Furthermore, Figure 4 displays that the distances of the variables from the origin in all covariates are relatively high, demonstrating that most of these variables are very useful for cluster analysis. The result further shows that the PET, elevation, and maximum and minimum temperatures have relatively high Cos2 values.

3.2. Climate Clusters of the Abbay River Basin

The unsupervised k-means clustering considered classifications using up to 150 clusters (Figure 5), from which the optimal number of clusters was selected using the elbow method. The Elbow method is a graphical quasi-objective method in which the optimal number of clusters is selected at the point where the graph of the number of clusters versus WCSS starts to bend and flatten out.

Based on the Elbow graph (Figure 5), 12 climate clusters were identified and mapped (Figure 6). The climate clusters are simply labeled by numbers from 1 to 12.
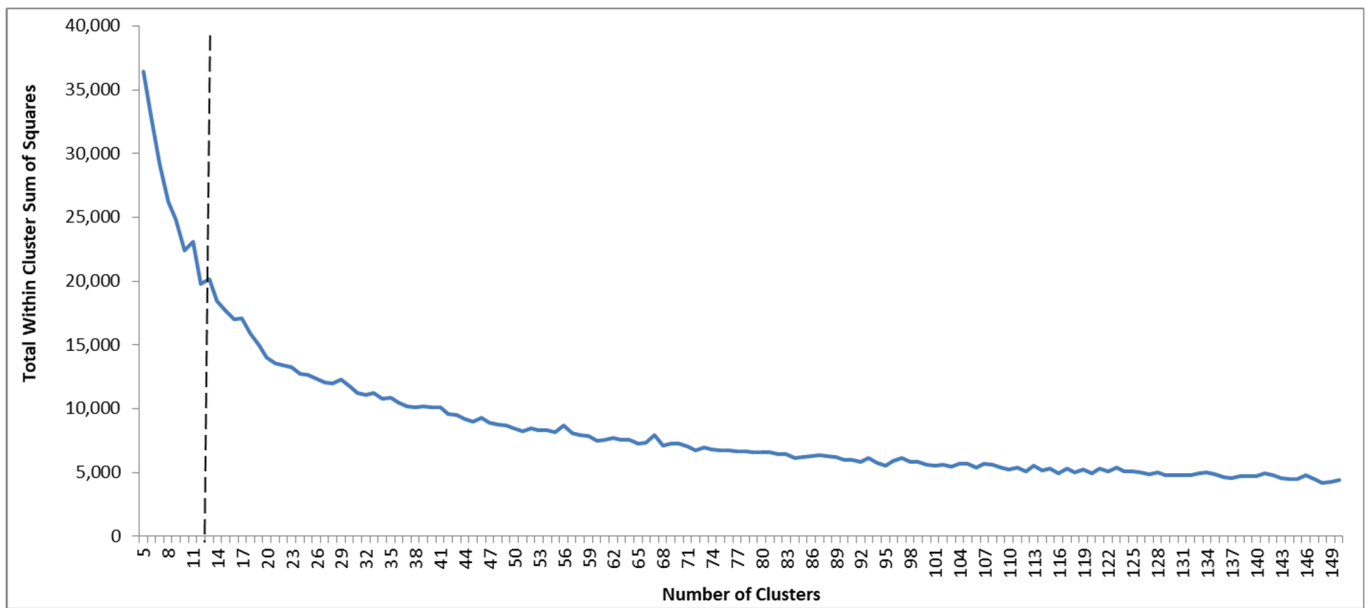
Figure 5. Total number of climate clusters generated by the k-means clustering and optimal number of clusters determined by the Elbow method. The broken line indicate the number of clusters determined by the Elbow method.
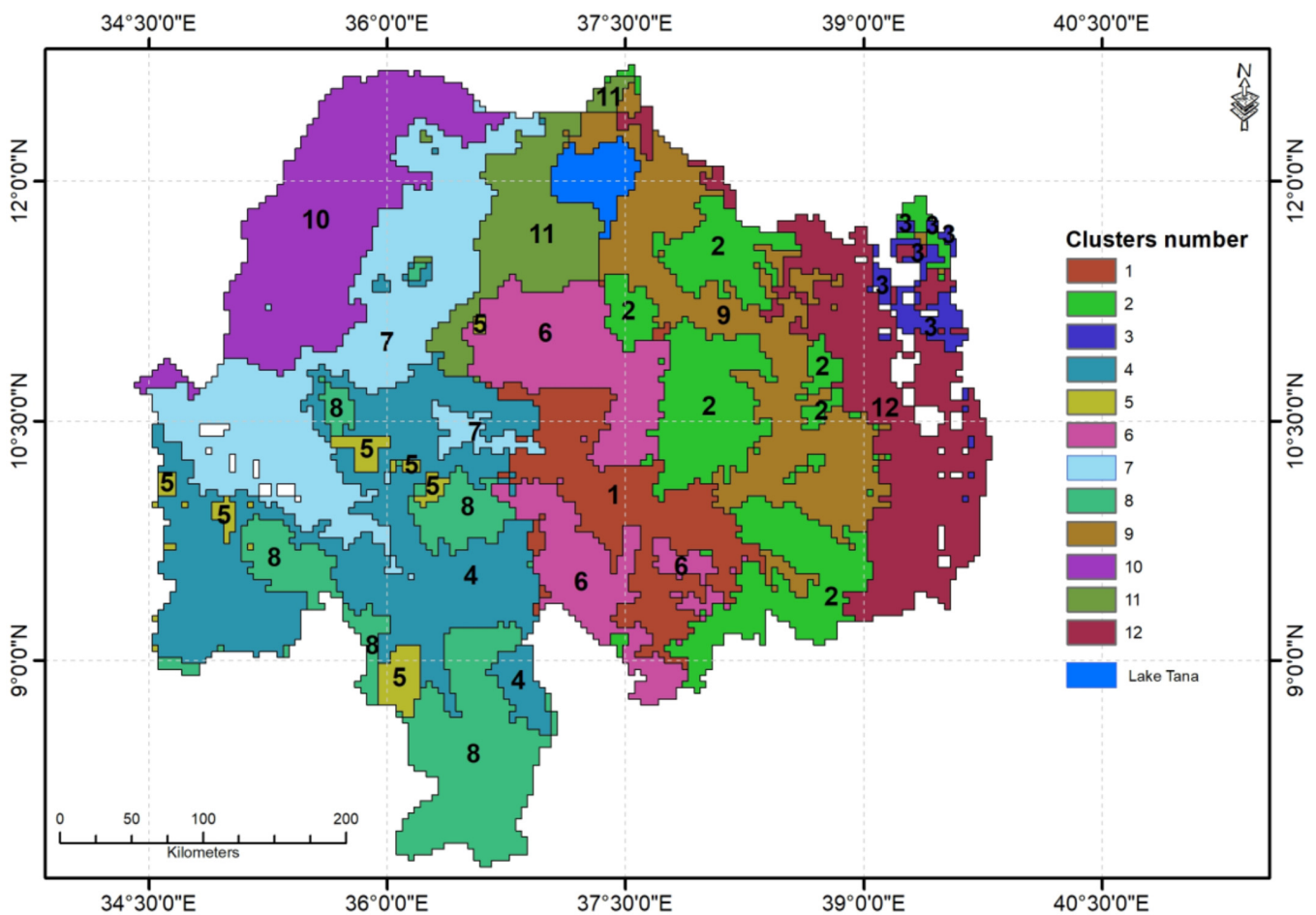

Figure 6. Climate clusters in the Abbay Basin generated by the k-means clustering method.

3.3. Climate Variation between Clusters

Table 2 presents the areal mean annual value of the climate variables for the 12 climate clusters of the Abbay River basin. The climate variables that were used for the study are important determinant factors of spatiotemporal variability and availability of green water for rain-fed agriculture.

Table 2. Characteristics of the climate variables in the 12 climate clusters.

Climate Clusters	Rainfall Onset Date (Pentad)	Rainfall Cessation Date (Pentad)	LGP (Pentad)	PCI	Annual Rainfall (mm)	PET (mm)	Soil Moisture (mm)	Min Tem. (°C)	Max Tem. (°C)	Mean Elevation (m asl)	Rainfall Cycle (number)
1	32.3	53.4	21.1	16.6	1386.4	1432.7	24.7	13.8	26.7	1561.9	1
2	33.8	53.6	19.8	18.1	1190.2	1261.2	13.4	9.2	23.1	2538.5	2
3	19.2	49.5	30.4	20.3	1006.3	1303.0	13.8	8.9	22.4	2620.3	2
4	26.1	54.3	28.2	16.2	1514.2	1425.6	62.5	14.5	28.7	1401.2	1
5	26.1	60.0	33.9	15.9	1603.8	1409.8	75.5	14.6	28.0	1458.7	1
6	31.8	53.7	21.9	16.2	1645.8	1289.1	33.5	10.8	24.3	2267.5	1
7	27.2	54.0	26.8	18.2	1423.5	1655.8	60.1	16.4	31.2	974.8	1
8	25.5	53.9	28.5	14.6	1769.5	1320.7	79.9	12.9	26.2	1846.8	1
9	33.6	53.7	20.0	19.9	1157.8	1467.0	10.6	12.4	27.0	1798.6	2
10	27.2	54.2	27.0	19.5	1198.9	1846.8	51.6	19.1	34.8	698.0	1
11	30.4	54.1	23.6	19.0	1427.5	1449.4	58.3	12.9	27.6	1755.9	1
12	34.4	49.2	14.8	21.1	1006.6	1301.3	11.5	9.0	22.0	2511.5	2

Note: Pentad is a period of five days.

The results demonstrate that four of the climate clusters (2, 3, 9, and 12) experience a bimodal (*Belg* and *Kiremt*) rainfall pattern and are located in the eastern part of the basin (Figure 6). The remaining eight clusters experience monomodal rainfall patterns or the *Kiremt* season only. The mean length of growing period (LGP) for the *Kiremt* season varies between 2.5 months in climate region 12 and 5.6 months in climate region 5. The climate regions located in the western part of the basin have relatively long growing periods (4.5–5.6 months). In contrast, the LGP was relatively short (3.3–3.9 months) for those climate regions located in the central and eastern parts of the basin, except for region three, where the LGP is 5.1 months. The relatively longer LGP for region three, which is located in the eastern part of the basin, is attributable to the early onset of rainfall. Rainfall in this region exceeds half of the PET in early March, while this occurs in early May in the other regions of the eastern and central parts of the basin.

The rainfall onset and cessation dates were earliest for region 3; in this region, rainfall exceeds half of the PET in early April and drops to half of PET in early September. Region 12 has a similar rainfall cessation date (early September). The rainfall onset time in five regions (4, 5, 7, 8, and 10) is in the first two weeks of May. The rainfall onset for the other six regions is between early May (regions 6 and 11) and the third week of May (regions 2, 9, and 12). The rainfall cessation date for four climate regions (1, 2, 6, and 9) is in the last week of September, while it is in early October in five regions (4, 7, 8, 10, and 11). The fall of rainfall amount to less than half of the PET can be caused by the decrease in rainfall amount or increase in the PET amount as the temperature starts to rise with the decreasing cloud cover over the region. The rainfall cessation time for region 5 is in October.

In general, the mean annual rainfall decreases from the southwestern towards the northern and northeastern parts of the basin. The mean annual rainfall is relatively small (less than 1200 mm) for climate regions 2, 3, 9, and 12, which are all located in the eastern and central parts of the basin. The mean annual rainfall is relatively high (1514.2–1769.5 mm) in four climate regions (4, 5, 6, and 8) which are located in the southwestern part of the basin. The mean annual rainfall in regions 7, 10, and 11, which are located in the northwestern part of the basin, is 1423.5 mm, 1198.9 mm, and 1427.5 mm, respectively. Furthermore, the mean annual rainfall for region 1 is 1386.4 mm.

The intensity of rainfall, as represented by PCI, is lowest (14.6 mm) in region 8 and highest (21.1 mm) in region 12. The PCI is relatively low (14.6–16.6) for regions 1, 4, 5, 6, and

8, and all of these regions are located in the southwestern part of the basin. These climate clusters are also known for their extended rainfall season. The PCI is high (19.9–21.1) in regions 3, 9, and 12; all of these regions are located in the extreme eastern part of the basin. The mean annual PET amount is lowest (1261.2 mm) in region 2 and highest (1846.8 mm) in region 10. In general, the mean annual PET is high in climate regions 7 (1655.8 mm) and 10 (1846.8 mm); both of these regions are located in the western lowland part of the basin. It is relatively low (1261.2–1301.3 mm) in regions 2, 3, 6, 8, and 12. The mean annual PET in the five regions (1, 4, 5, 9, and 11) varies between 1409.8 mm and 1467.0 mm. The spatial variation of annual PET is due to the variation of temperature between the climate clusters. The mean annual minimum and maximum temperatures vary between 8.9 °C and 19.1 °C and 22.0 °C and 34.8 °C, respectively. The mean minimum and maximum temperatures are high in the two climate regions (7 and 10) that are located in the western part of the basin. The mean minimum and maximum temperatures are 16.4 °C and 31.2 °C in region 7 and 19.1 °C and 34.8 °C in region 10, respectively. Low mean minimum (8.9–9.2 °C) and maximum (22.0–23.1 °C) temperatures characterize the three climate regions, which are located in the eastern part of the basin.

Soil moisture content also reveals significant variation between the climate clusters. The lowest (10.6 mm) mean annual soil moisture content is found for climate region 9, and the highest (79.9 mm) mean annual soil moisture content is found for climate region 8. In general, the mean annual soil moisture content is relatively high (60.1–79.9 mm) in four climate regions (4, 5, 7, and 8). In contrast, four climate regions that include regions 2, 3, 9, and 12 have relatively low (10.6–13.8 mm) mean soil moisture content; all of these regions are located in the eastern part of the Abbay basin. The mean annual soil moisture content for the other climate regions varies between 24.7 mm in region 1 and 58.3 mm in region 11.

The mean altitude of climate regions varied between 698 m asl for climate region 10 and 2620.3 m asl for climate region 3 (Table 2). As shown in Table 2, the mean altitudes for climate regions 7 and 10 are relatively low at 974.8 m asl and 698 m asl, respectively. Both of these climate regions are located in the northwestern part of the basin. In contrast, climate regions 2, 3, 6, and 12, which are located in the eastern part of the basin, have relatively high ranges from 2267.2 m asl and 2620.3 m asl. The results further showed the absence of a systematic relationship between rainfall variables and altitude in the Abbay basin. In contrast, the distribution of PET, temperature, and soil moisture displayed a systematic relationship with altitude. In this regard, temperature and PET are relatively higher in lowland climate regions (7 and 10) and low in highland climate regions (e.g., 2, 3, 9, and 12). On the other hand, the mean annual soil moisture amount is relatively high in the lowland climate regions (7 and 10) and relatively low in highland climate regions (e.g., 2, 3, 9, and 12).

In general, regions 2, 3, 9, and 12 have two rain cycles; most of the climate characteristics are relatively similar, except climate region 3 has early rainfall onset and longer LGP, and climate region 9 has higher temperature values. Of the others, climate region 5 is distinct as it has a relatively longer LGP, which is attributed to the late cessation date. On the other hand, climate region 10, followed by climate region 7, has a high PET. Furthermore, climate regions 1 and 6 are very similar in all rainfall characteristics, except climate region 6 is slightly wetter. Similarly, all the rainfall indicators and PET amounts are relatively similar for climate regions 2 and 9.

4. Implications for Targeting Green Water Management Technologies

This study produced data-driven homogenous climate clusters that are useful for identifying local scale climate-induced risks for rain-fed agriculture systems and for facilitating the selection of site-specific green water management technologies in the Abbay River basin. The assumption is that spatiotemporal climate variability is the leading environmental determinant factor to the productivity of rain-fed agriculture in the basin. Climate variability controls the practice and productivity in the rain-fed agricultural system by determining the start and end of the farming calendar, LGP, soil moisture balance, and types of crops that

can be grown in an area. It also relates to many risks to rain-fed agriculture, such as shortage of water associated with seasonality of the rainfall or due to excessive evapotranspiration or both, the occurrence of flood and soil erosion due to a high amount or intensity of rainfall or both, water logging and soil acidity caused by the seasonal high-intensity rainfall, and soil salinity caused by high rates of evapotranspiration. These risks can significantly constrain rain-fed agricultural practices and crop productivity [2,5,7,9,41,42]. It is important to note that the prevalence, severity, and effects of these climate variability-induced agricultural challenges vary spatially across the Abbay basin [16]. Previous soil and water conservation practices, as well as other agronomic interventions, did not achieve the intended outcomes as they followed a one-size-fits-all top-down approach without considering regional and local-scale climate variability [17,32].

The results generated from this study have contributed to identifying appropriate green water management technologies to address climate-induced risks to the rain-fed agricultural system. For example, all climate regions located in the eastern part of the basin, except climate region three, have relatively short LGP (2.5–3.9 months), which means longer dry periods. This suggests that agricultural productivity in these regions is constrained by the short LGP. Some of the climate regions (2, 9, and 12) experience a bimodal (*Kiremt* and *Belg*) rainfall pattern; the rainfall amount during the later season is too erratic, unreliable, and exceeded by PET. In these regions, rainwater harvesting and supplementary irrigation can be used to complement the short LGP and improve agricultural productivity.

Climate regions 2, 9, 11, and 12 have relatively high PCI (18.1–21.1), which means there is high rainfall seasonality that can generate excessive surface runoff during the *Kiremt* season. Rainwater harvesting, such as small-scale water reservoirs and well-designed private ponds, is a useful strategy to extend the period of water availability in these regions. Using water-efficient technologies and agronomic practices are also appropriate interventions in these regions. It is important to note that most of these areas have dense populations, which means a large number of the workforce remains idle for an extended period (6.5–7.5 months) of the year. Rainwater harvesting and dry season production activities are therefore important from the perspective of improved use of labor resources.

Many empirical studies confirm the significant contribution of small-scale irrigation to poverty reduction [43–46] and improved food security [47–49] in the rural areas of Ethiopia. Furthermore, the construction of rainwater harvesting schemes in regions that experience short LGP and high PCI can reduce the frequency and intensity of flood events during the peak rainfall season and increase groundwater storage and low flows. The presence of a water harvesting scheme at an upper part of the river basin can significantly regulate soil erosion and reduce sediment yields [50].

Soil management practices emerge as priority interventions in climate regions 2, 3, 9, 11, and 12, where the PCI is high. This is because high rainfall concentration results in low infiltration and high surface runoff, causing severe soil erosion [16]. Soil acidity management should be a top priority green water management strategy in climate regions 4, 5, 6, and 8, where annual rainfall amount is in excess of 1500 mm.

For climate regions 2, 3, 9, and 12 (all located in the eastern part of the basin), where soil moisture contents are low (10.6–13.8 mm), soil water conservation technologies are important interventions. Although these climate regions have bimodal rainfall cycles (*Kiremt* and *Belg*), the *Kiremt* rainfall has a short duration (2.5–3.3 months), except for region 3, where the LGP is 5.1 months, and the *Belg* season's rainfall is decreasing and highly unreliable for agricultural production. A recent study by Tibebe [16] indicated that agricultural productivity in the Abbay basin is negatively affected not only by the high level of climate variability but also by the low and poor utilization and management of the available water. Hence, it is important to enhance or introduce water utilization technologies to efficiently use the available moisture that occurs during the two rainy seasons. There are very large areas in region 12, particularly in Semien Shewa and Debub Wollo, where farmers cannot cultivate crops during the *Kiremt* season due to water logging [51]. This problem is observed in the highland areas, where barley is the dominant type of crop. The

water logging problem is not only caused by the occurrence of excessive rainfall but also by the nature of the soil. Therefore, water logging management should be a top priority green water management issue in these areas.

Opportunities extend the crop season using available moisture in those climate regions that have relatively long LGP (3, 4, 5, 7, 8, and 10). The LGP in these climate regions varies between 4.5 and 5.6 months, and all except region 3 are located in the western part of the basin. It is important to target short-maturing crop varieties and other agronomic and agro-climate services to enable crop production for more than a single season.

The climate regions 2 and 9 experience short LGP, heavy rainfall during the *kiremt* season, soil erosion, and shortage of soil moisture in the dryland areas. Hence, the impact of such multiple risks on the rain-fed agriculture should be addressed by carefully understanding their co-occurrences and synergies and through targeted package-based interventions. For example, structural measures used to protect soil erosion in moisture-stressed highland areas can be designed in a way to enhance on-farm soil moisture and groundwater recharge by reducing the velocity of surface runoff.

5. Conclusions

Clustering a given geographic region into homogenous climate units is important to identify site-specific climate-related water security risks and facilitate the selection and implementation of appropriate green water management technologies for improved productivity of rain-fed agricultural systems. This study undertook a climate classification scheme for the Abbay basin, where rain-fed agriculture is highly constrained by spatiotemporal climate variability. The k-means unsupervised clustering approach was employed to define homogeneous climate clusters by using climate variables (daily rainfall amount, rainfall intensity, rainfall onset and cessation dates, LGP, PCI, PET, and soil moisture) that have determinant impacts on rain-fed agriculture.

The climate classification scheme generated 12 homogenous climate clusters for the basin. The results are discussed with reference to climatic characteristics, potential climate-related risks to rain-fed agriculture, and green water management options across the identified climate clusters. The climate classification approach and results presented in this study have multiple implications for transformative green water management by facilitating the selection and targeted implementation of technologies tailored to local circumstances. The overall outcome is the efficient utilization of the scarce water and land resources and improved agricultural production and food security in the area. Furthermore, the study provides a methodological framework that can be used in the other river basins of Ethiopia and, indeed, elsewhere.

References

1. Brown, C.; Hansen, J.W. *Agricultural Water Management and Climate Risk. Report to the Bill and Melinda Gates Foundation*; IRI Tech. Rep. No. 08-01; International Research Institute for Climate and Society: Palisades, NY, USA, 2008; p. 19.

2. Kotir, J.S. Climate change and variability in Sub-Saharan Africa: A review of current and future trends and impacts on agriculture and food security. *Environ. Dev. Sustain.* **2010**, *13*, 587–605. [CrossRef]

3. Holleman, C.; Rembold, F.; Crespo, O.; Conti, V. The impact of climate variability and extremes on agriculture and food security—An analysis of the evidence and case studies. In *Background Paper for The State of Food Security and Nutrition in the World*; FAO Agricultural Development Economics Technical Study No. 4; FAO: Rome, Italy, 2018. [CrossRef]

4. Conway, D.; Schipper, E.L.F. Adaptation to climate change in Africa: Challenges and opportunities identified from Ethiopia. *Glob. Environ. Chang.* **2011**, *21*, 227–237. [CrossRef]

5. Ademe, F.; Kibret, K.; Beyene, S.; Getinet, M.; Mitike, G. Rainfall analysis for rain-fed farming in the Great Rift Valley Basins of Ethiopia. *J. Water Clim. Chang.* **2020**, *11*, 812–828. [CrossRef]

6. Ademe, D.; Zaitchik, B.F.; Tesfaye, K.; Simane, B.; Alemayehu, G.; Adgo, E. Analysis of agriculturally relevant rainfall characteristics in a tropical highland region: An agroecosystem perspective. *Agric. For. Meteorol.* **2021**, *311*, 108697. [CrossRef]

7. Mubenga-Tshitaka, J.; Dikgang, J.; Mwamba, J.W.M.; Gelo, D. Climate variability impacts on agricultural output in East Africa. *Cogent Econ. Financ.* **2023**, *11*, 2181281. [CrossRef]

8. Ochieng, J.; Kirimi, L.; Mathenge, M. Effects of climate variability and change on agricultural production: The case of small scale farmers in Kenya. *NJAS Wagening. J. Life Sci.* **2016**, *77*, 71–78. [CrossRef]

9. Bewket, W. Climate change perceptions and adaptive responses of smallholder farmers in central highlands of Ethiopia. *Int. J. Environ. Stud.* **2012**, *69*, 507–523. [CrossRef]

10. Evangelista, P.; Young, N.; Burnett, J. How will climate change spatially affect agriculture production in Ethiopia? Case studies of important cereal crops. *Clim. Chang.* **2013**, *119*, 855–873. [CrossRef]

11. Ginbo, T. Heterogeneous impacts of climate change on crop yields across altitudes in Ethiopia. *Clim. Chang.* **2022**, *170*, 12. [CrossRef]

12. Tamene, L.; Abera, W.; Bendito, E.; Erkossa, T.; Tariku, M.; Sewnet, H.; Tibebe, D.; Sied, J.; Feyisa, G.; Wondie, M.; et al. Data-driven similar response units for agricultural technology targeting: An example from Ethiopia. *Exp. Agric.* **2022**, *58*, e27. [CrossRef]

13. Zang, C.; Liu, J.; van der Velde, M.; Kraxner, F. Assessment of spatial and temporal patterns of green and blue water flows under natural conditions in inland river basins in Northwest China. *Hydrol. Earth Syst. Sci.* **2012**, *16*, 2859–2870. [CrossRef]

14. Zhang, Y.; Tang, C.; Ye, A.; Zheng, T.; Nie, X.; Tu, A.; Zhu, H.; Zhang, S. Impacts of climate and land-use change on blue and green water: A case study of the upper Ganjiang River Basin, China. *Water* **2020**, *12*, 2661. [CrossRef]

15. Lyu, L.; Wang, X.; Sun, C.; Ren, T.; Zheng, D.-F. Quantifying the Effect of Land Use Change and Climate Variability on Green Water Resources in the Xihe River Basin, Northeast China. *Sustainability* **2019**, *11*, 338. [CrossRef]

16. Tibebe, D.; Teferi, E.; Bewket, W.; Zeleke, G. Climate induced water security risks on agriculture in the Abbay river basin: A review. *Front. Water* **2022**, *4*, 961948. [CrossRef]

17. Zimale, F.A.; Tilahun, S.A.; Tebebu, T.Y.; Guzman, C.D.; Hoang, L.; Schneiderman, E.M.; Langendoen, E.J.; Steenhuis, T.S. Improving watershed management practices in humid regions. *Hydrol. Process.* **2017**, *31*, 3294–3301. [CrossRef]

18. FAO. *Agro-Ecological Zoning Guidelines*; FAO Soils Bulletin 73, Soil Resources, Management and Conservation Service, FAO Land and Water Development Division; Food and Agriculture Organization of the United Nations: Rome, Italy, 1996; p. 78, ISBN 92-5-103890-2.

19. BCEOM. *Abbay River Basin Integrated Development Master Plan-Phase 2—Data Collection—Site Investigation Survey and Analysis—Volume I—Natural Resources—Geology; Ministry of Water Resource*; BCEOM: Addis Ababa, Ethiopia, 1998; p. 144.

20. Cheung, W.H.; Senay, G.B.; Singh, A. Trends and spatial distribution of annual and seasonal rainfall in Ethiopia. *Int. J. Climatol.* **2008**, *28*, 1723–1734. [CrossRef]

21. Mengistu, D.; Bewket, W.; Lal, R. Recent spatiotemporal temperature and rainfall variability and trends over the Upper Blue Nile River Basin, Ethiopia. *Int. J. Climatol.* **2014**, *34*, 2278–2292. [CrossRef]

22. Degefu, M.A.; Rowell, D.; Bewket, W. Teleconnections between Ethiopian rainfall variability and global SSTs: Observations and methods for model evaluation. *Meteorol. Atmos. Phys.* **2017**, *129*, 173–186. [CrossRef]

23. Degefu, M.A.; Tadesse, Y.; Bewket, W. Observed changes in rainfall amount and extreme events in southeastern Ethiopia, 1955–2015. *Theor. Appl. Climatol.* **2021**, *144*, 967–983. [CrossRef]

24. Degefu, M.A.; Bewket, W.; Amha, Y. Evaluating performance of 20 global and quasi-global precipitation products in representing drought events in Ethiopia: Visual analysis. *Weather Clim. Extrem.* **2022**, *35*, 100416. [CrossRef]

25. Abdisa, T.B.; Diga, G.M.; Tolessa, A.R. Impact of climate variability on rain-fed maize and sorghum yield among smallholder farmers. *Cogent Food Agric.* **2022**, *8*, 2057656. [CrossRef]

26. Desta, G.; Kassawmar, T.; Tadesse, M.; Zeleke, G. Extent and distribution of surface soil acidity in the rainfed areas of Ethiopia. *Land Degrad. Dev.* **2021**, *32*, 5348–5359. [CrossRef]

27. Abate, E.; Hussein, S.; Laing, M.; Mengistu, F. Soil acidity under multiple land-uses: Assessment of perceived causes and indicators, and nutrient dynamics in small-holders' mixed-farming system of northwest Ethiopia. *Acta Agric. Scand. B Soil Plant Sci.* **2017**, *67*, 134–147. [CrossRef]

28. Bedane, H.R.; Beketie, K.T.; Fantahun, E.E.; Feyisa, G.L.; Anose, F.A. The impact of rainfall variability and crop production on vertisols in the central highlands of Ethiopia. *Environ. Syst. Res.* **2022**, *11*, 26. [CrossRef]

29. Hasanuzzaman, M.; Nahar, K.; Alam, M.M.; Roychowdhury, R.; Fujita, M. Physiological, biochemical, and molecular mechanisms of heat stress tolerance in plants. *Int. J. Mol. Sci.* **2013**, *14*, 9643–9684. [CrossRef] [PubMed]

30. Erkossa, T.; Awulachew, S.B.; Haileslassie, A.; Yilma, A.D. Impacts of improving water management of smallholder agriculture in the upper Blue Nile Basin. In *CP 19 Project Workshop Proceedings*; IWMI: Addis Ababa, Ethiopia, 2009; Available online: https://publications.iwmi.org/pdf/H042504.pdf (accessed on 12 September 2022).

31. Fazzini, M.; Bisci, C.; Billi, P. The Climate of Ethiopia. In *Landscapes and Landforms of Ethiopia, World Geomorphological Landscapes*; Billi, P., Ed.; Springer Science + Business Media: Dordrecht, The Netherlands, 2015. [CrossRef]

32. Tebebu, T.Y.; Bayabil, H.K.; Stoof, C.R.; Giri, S.K.; Gessess, A.A.; Tilahun, S.A.; Steenhuis, T.S. Characterization of degraded soils in the humid Ethiopian Highlands. *Land Degrad. Develop.* **2017**, *28*, 1891–1901. [CrossRef]

33. Dinku, T.; Hailemariam, K.; Maidment, R.; Tarnavsky, E.; Connor, S. Combined use of satellite estimates and rain gauge observations to generate high-quality historical rainfall time series over Ethiopia. *Int. J. Climatol.* **2014**, *34*, 2489–2504. [CrossRef]

34. Romano, N.; Palladino, M.; Chirico, G.B. Parameterization of a bucket model for soil-vegetation-atmosphere modeling under seasonal climatic regimes. *Hydrol. Earth Syst. Sci.* **2011**, *15*, 3877–3893. [CrossRef]

35. Mao, W.; Yang, J.; Zhu, Y.; Ye, M.; Liu, Z.; Wu, J. An efficient soil water balance model based on hybrid numerical and statistical methods. *J. Hydrol.* **2018**, *559*, 721–735. [CrossRef]

36. Oliver, J.E. Monthly precipitation distribution: A comparative index. *Prof. Geogr.* **1980**, *32*, 300–309. [CrossRef]

37. Kaiser, H.F.; Rice, J. Little jiffy, mark IV. Educ. *Psychol. Meas.* **1974**, *34*, 111–117. [CrossRef]

38. Jain, A.K.; Duin, R.P.W.; Mao, J. Statistical pattern recognition: A review. *IEEE Trans. Pattern Anal. Mach.* **2000**, *22*, 4–37. [CrossRef]

39. Rahmani, M.K.I.; Pal, N.; Arora, K. Clustering of image data using K-means and fuzzy K-means. *Int. J. Adv. Comput. Sci. Appl.* **2014**, *5*, 160–163.

40. Hot, E.; Popović-Bugarin, V. Soil data clustering by using K-means and fuzzy K-means algorithm. In Proceedings of the 2015 23rd Telecommunications Forum Telfor (TELFOR), Belgrade, Serbia, 24–26 November 2015; pp. 890–893.

41. Shukla, R.K.; Agrawal, J.; Sharma, S.; Chaudhari, N.S.; Shukla, K.K. (Eds.) *Social Networking and Computational Intelligence: Proceedings of SCI-2018*; Springer Nature Singapore Pte Ltd.: Singapore, 2020; Volume 100.

42. Zeweld, W.; Huylenbroeck, G.V.; Hidgot, A.; Chandrakanth, M.; Speelman, S. Adoption of small-scale irrigation and its livelihood impacts in Northern Ethiopia. *Irrigat. Drain.* **2015**, *64*, 655–668. [CrossRef]

43. Mengistie, D.; Kidane, D. Assessment of the impact of small-scale irrigation on household livelihood improvement at Gubalafto District, North Wollo, Ethiopia. *Agriculture* **2016**, *6*, 27. [CrossRef]

44. Abebe, A. The determinants of small-scale irrigation practice and its contribution on household farm income: The case of Arba Minch Zuria Woreda, Southern Ethiopia. *Afr. J. Agric. Res.* **2017**, *12*, 1136–1143.

45. Kassie, K.E.; Alemu, B.A. Does irrigation improve household's food security? The case of Koga irrigation development project in northern Ethiopia. *Food Secur.* **2021**, *13*, 291–307. [CrossRef]

46. Assefa, E.; Ayalew, Z.; Mohammed, H. Impact of small-scale irrigation schemes on farmers livelihood, the case of Mekdela Woreda, North-East Ethiopia. *Cogent Econ. Finan.* **2022**, *10*, 2041259. [CrossRef]

47. Wondimagegnhu, B.A.; Bogale, B.A. Small-scale irrigation and its effect on food security of rural households in North-West Ethiopia: A comparative analysis. *Ethiop. J. Sci. Technol.* **2020**, *13*, 31–51. [CrossRef]

48. Jambo, Y.; Alemu, A.; Tasew, W. Impact of small-scale irrigation on household food security: Evidence from Ethiopia. *Agricu. Food Secur.* **2021**, *10*, 21. [CrossRef]

49. Maru, H.; Haileslassie, A.; Zeleke, T. Impacts of small-scale irrigation on farmers' livelihood: Evidence from the drought prone areas of upper Awash sub-basin, Ethiopia. *Heliyon* **2023**, *16*, e16354. [CrossRef] [PubMed]

50. Dile, Y.T.; Karlberg, L.; Daggupati, P.; Srinivasan, R.; Wiberg, D.; Rockström, J. Assessing the implications of water harvesting intensification on upstream-downstream ecosystem services: A case study in the Lake Tana basin. *Sci. Total Environ.* **2016**, *542*, 22–35. [CrossRef] [PubMed]

51. Gebrehiwot, K.A. A review on waterlogging, salinization and drainage in Ethiopian irrigated agriculture. *Sustain. Water Resour. Manag.* **2018**, *4*, 55–62. [CrossRef]